Metastable, Partially Depolymerized Xanthans and Rearrangements toward Perfectly Matched Duplex Structures

Bjørn E. Christensen,*,† Olav Smidsrød,† and Bjørn T. Stokke‡

Norwegian Biopolymer Laboratory, Departments of Biotechnology and of Physics and Mathematics, Norwegian University of Science and Technology, N-7034 Trondheim, Norway

Received September 26, 1995; Revised Manuscript Received January 11, 1996[⊗]

ABSTRACT: The depolymerization of double-stranded xanthan by H_2O_2/Fe^{2+} (at 20 °C) leads to the formation of a metastable duplex stabilized by partially overlapping chains. A heat treatment well above the conformational melting temperature, T_m, followed by cooling below T_m resulted in a relatively large decrease in the weight average molecular weight, $\bar{M}_w$, as shown by size exclusion chromatography. A corresponding decrease in the contour length of the individual duplexes was demonstrated by electron microscopy. The decrease is primarily ascribed to a rearrangement of chain fragments which dissociate from the duplexes ($T \geq T_m$) and reassociate to form more perfectly matched duplexes upon cooling below T_m. The decrease in $\bar{M}_w$ was most pronounced (factor 7−9) for slightly depolymerized xanthan whereas this factor decreased for more extensively depolymerized xanthan. A second heat treatment did not result in any further change in the molecular weight distribution, indicating that depolymerization did not occur to any significant extent. The experimental results were fairly well reproduced by a Monte Carlo simulation, where the duplex stability is governed by the degree of chain scission (α) and the critical degree of polymerization (DP_c) needed for maintaining a stable duplex. For xanthan partially degraded by acid hydrolysis at high temperatures we suggest that the relatively small decrease in $\bar{M}_w$ (factor 1.3−1.5) upon heat treatment well above T_m is because a certain rearrangement toward perfectly matched duplexes occurred during the hydrolysis. This is partly ascribed to the larger DP_c prevailing under the depolymerization conditions and partly because chain rearrangements are kinetically facilitated at high temperatures.

Introduction

The bacterial polysaccharide xanthan (Figure 1) is used commercially in a variety of applications, for instance as an effective viscosifier of aqueous solutions. Among many useful properties is its enhanced stability toward degradation (loss of viscosity) as compared to several other polysaccharides (*e.g.* cellulose derivatives) or water soluble synthetic polymers (*e.g.* partially hydrolyzed polyacrylamides).[1] This property is associated with the ordered, double-stranded (duplex) state, whereas heating above the conformational transition temperature (T_m) to induce the partially or fully dissociated duplex leads to a large increase in the rate of depolymerization when measured as loss of viscosity or decrease in molecular weight.[2,3] In contrast, the rate of cleavage of glycosidic linkages in the glucan backbone does *not* seem to depend strongly on the conformational state.[4]

The random depolymerization of double-stranded xanthan has been investigated both experimentally[3−9] and theoretically.[5] A basic feature is the conservation of the duplex structure early in the degradation, whereas a substantial increase in the apparent degradation rate, measured as a decrease in molecular weight or viscosity, occurs in later stages.[3] It is assumed that the duplex initially may tolerate several scissions in the individual chains without a corresponding decrease in molecular weight. The duplex may thus contain "internal" chain breaks, as shown schematically in Figure 2 (structure B). This structure is therefore stabilized by overlapping chain ends. The pairwise association of individual chains to form the duplex state is expected to be a cooperative process, and a dependence on the DP for

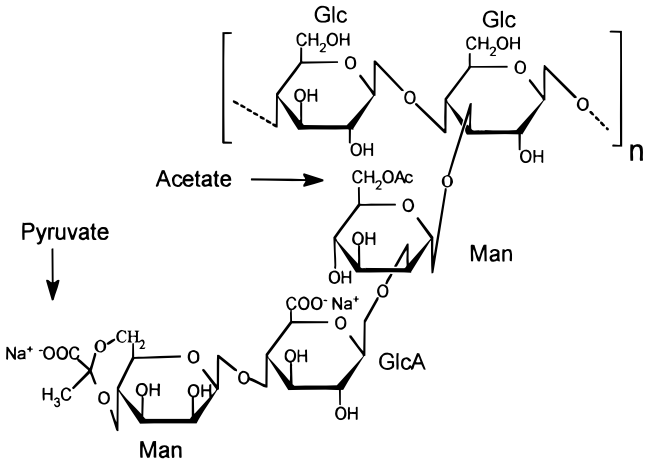

Figure 1. Pentasaccharide repeating unit of xanthan. Abbreviations: Glc, D-glucose; GlcA, D-glucuronic acid; Man, D-mannose. Note that in the samples studied here most of the acetate and pyruvate substituents have been removed prior to further treatments in order to obtain a sharper order−disorder transition.

overlapping regions can be predicted[10] from, *e.g.*, the nonstaggered zipper model for pairwise associating polymers.[11] Such theories predict that when DP goes below a critical value (DP_c), duplex dissociation occurs, either by breaking in two individual duplexes by dissociation of overlapping chains or by the release of a single-stranded fragment when adjacent breaks occur in the same strand (Figure 2). The latter process is particularly easily monitored by, *e.g.*, size-exclusion chromatography[4,7] or by gel filtration.[7]

These principles were applied in a Monte Carlo analysis developed to give a quantitative kinetic description of the random depolymerization of single-stranded and multistranded polymers,[5] where it was inherently assumed that the duplex remained intact except when chain fragments and chain overlaps were

* To whom all correspondence should be addressed.
† Department of Biotechnology.
‡ Department of Physics and Mathematics.
⊗ Abstract published in *Advance ACS Abstracts,* March 15, 1996.

0024-9297/96/2229-2939$12.00/0

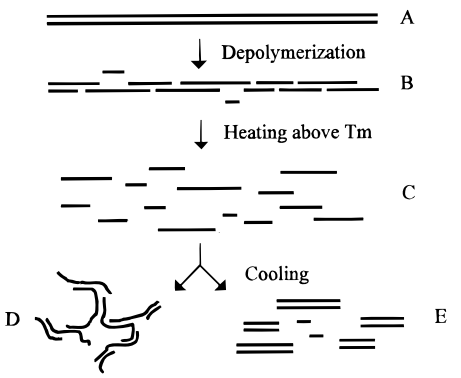

Figure 2. Schematic representation of the depolymerization of double-stranded xanthan (A−B). Side chains attached to every second glucose residue are omitted for clarity. The duplex structure is stabilized by segment−segment interactions between residues in adjacent chains (not depicted). Random depolymerization will induce a metastable structure (B) consisting of overlapping chain fragments and a fraction of short fragments ($DP < DP_c$) unable to remain incorporated in a duplex. A subsequent heat treatment well above T_m results in partial or complete dissociation of the duplexes. Complete dissociation results in dispersed single strands of various lengths (C). The cooling step may either induce an aggregated state (D) or perfectly matched duplexes (E), largely depending on the polymer concentration.

equal to, or lower than, DP_c, where duplex scission or a release of a single-stranded fragment occurred, respectively. Two central features predicted by the model, an initial period with minimal decrease in $\bar{M}_w$ followed by a transition toward a regime where $\bar{M}_w \sim t^{-\nu}$, were verified experimentally for acid hydrolysis.[5,7] However, the predicted value of the exponent ν (1.66) was exceeded for long degradation times, presumably because of an inherent increase in the rate of hydrolysis. The value of DP_c could be estimated from the relative content of single-stranded fragments at different degrees of depolymerization, expressed as $\bar{M}_w/\bar{M}_{w,0}$.[7]

The postulated structures (Figure 2, structure type B) are clearly not in their thermodynamically most stable state. A redistribution of chain fragments to form perfectly matched duplexes (Figure 2, structure type E) is favored because of the enthalpy reduction, by forming a larger number of favorable chain−chain interactions, and because of the entropy gain by forming a larger number of species. The quantitative relations between, *e.g.*, $\bar{M}_w$ and the degree of chain scission (α) predicted previously in the Monte Carlo analysis[5] does not take such redistributions into account, and the analysis is therefore extended here. The major effect of a redistribution is expected to be a decrease in $\bar{M}_w$. This decrease is expected to depend on $\bar{M}_w$, α, and DP_c, as will be discussed below.

The existence of metastable xanthan duplexes (Figure 2, type B) is suggested by the fact that the depolymerization of double-stranded xanthan largely adheres to the Monte Carlo model,[5,7] with respect to both the initial stabilization and the release of conformationally disordered fragments of low molecular weight. It has further been noted that a heat treatment (above T_m) of partially depolymerized xanthan in dilute solution resulted in a large and irreversible reduction of viscosity,[12] which can be explained by a redistribution process, although other phenomena, in particular aggregation and thermal degradation, cannot be excluded *a priori*.

The question of chain redistribution is also related to, *e.g.*, formation and disintegration of aggregates and networks, annealing processes, or in more general terms, the modes of association of polymer chains. These seem to vary considerably, depending on the actual conditions. For example, heat treatment above T_m at relatively high xanthan concentrations, particularly above the critical overlap concentration (c^*), followed by cooling below T_m has been reported[13] to induce a more gel-like rheology. This was attributed[13] to the formation of a network stabilized by overlapping duplex regions (Figure 2, structure type D). It is expected that the formation of perfectly matched duplexes is largely favored at low concentrations, and heat treatment (*e.g.* autoclaving) is sometimes used to enhance the solubilization of xanthan to yield optically clear solutions.[14,15] The redistribution to presumably more stable states at low polymer concentrations has been observed with triple-stranded scleroglucan and schizophyllan. When the triple-stranded structure is completely dissociated into single strands, *e.g.* in DMSO, a renaturation (dialysis against water) at low polymer concentrations results not only in linear triple strands and aggregated forms but also, for sufficiently long chains, circular, triple-stranded species.[16,17] These forms are thermodynamically more stable than the corresponding linear species because of the higher degeneracy (higher entropy) introduced by allowing the individual chains in the circular triplex to adopt a multitude of relative positions, whereas for linear triplexes the chain ends should be perfectly matched.[16,17]

Analysis of the formation of reducing end groups within the glucan backbone has suggested that partially depolymerized xanthan contains a relatively high number of unexposed chain breaks,[4] in accordance with type B structures (Figure 2). However, a closer examination showed that the end groups were mainly confined to the fraction consisting of released single-stranded fragments,[7] and the number of end groups in the remaining duplex fraction could not be directly determined.

In the present study we investigate the possible existence of metastable "type-B" structures in partially depolymerized xanthans by exposing them to a thermal treatment at low polymer concentration. Two different polymer concentrations (below c^*) are used to investigate possible concentration effects. The treatment involves autoclaving (120 °C, 15 min) followed by a second treatment at 80 °C (60 min) and subsequently cooling to room temperature. At the ionic strength used (10 mM NaCl), T_m is near 60 °C for all of the samples.[4,6,7] The molecular weight and molecular weight distribution before and after the heat treatment is investigated by size-exclusion chromatography.[4,7] The samples studied were either depolymerized by acid hydrolysis (at 80 °C)[3,6,7] or by degradation with H_2O_2/Fe^{2+} (at 20 °C)[4,9] prior to the heat treatment. It should be noted that the depolymerization in *both* cases was performed in the fully ordered (double-stranded) conformation, even for acid hydrolysis (0.1 M HCl) at 80 °C because the low pH itself stabilizes the ordered state.[3] The changes in the structure and distribution of the side chains occurring in the degradation have been shown to have little influence on the macromolecular properties[4,7] and is therefore not considered here. Also included are xanthans depolymerized by ultrasonic irradiation. Such treatment is believed to produce fragments with a matched duplex structure. To examine the extent of thermal degradation during the heat treatment, a repeated treatment is in one case performed. In addition, a single-stranded polysaccharide (alginate) is included as a control, since in this case the decrease in

$\bar{M}_w$ directly reflects the extent of depolymerization. For the xanthans degraded by H_2O_2/Fe^{2+} analyses of reducing ends are included for the same reason.

The untreated and heat-treated samples were analyzed by size-exclusion chromatography (SEC), yielding the molecular weight distributions (MWD). Because of the low polymer concentrations and low molecular weights, in-line low angle laser light scattering (LALLS) detection could not be used for the majority of the samples. Instead, calculations of MWD and $\bar{M}_w$ were performed by using the relationship between M and elution volume established earlier.[4] The extent of redistribution of fragments is estimated by extending the previously described Monte Carlo analysis.[5] Independent information about the macromolecular properties is obtained by electron microscopy.[18,19]

Experimental Section

Samples. Xanthan was purified as described previously[4,7] and degraded by partial acid hydrolysis[3,7] (0.1 M HCl, 80 °C) for various times (up to 199 h) or by degradation with H_2O_2/Fe^{2+} (20 °C).[4] Ultrasonically depolymerized xanthan was prepared as described earlier.[20] Alginate samples included an algal alginate (LF 10/60) obtained from Pronova Biopolymer (Drammen, Norway) and a high molecular weight bacterial alginate (95% D-mannuronic acid) isolated[21] from *Pseudomonas aeruginosa*. All samples were freeze-dried except for the xanthans degraded with H_2O_2/Fe^{2+}, which were kept in aqueous solution (10 mM NaCl) following the degradation.

Heat Treatment. Solutions at two different xanthan concentrations (0.7 and 0.07 mg/mL) in 10 mM NaCl (total volume 0.5−1 mL) were transferred to 1 mL vials equipped with Teflon-faced septa and screw caps. The samples were autoclaved at 120 °C for 15 min with the caps loosely tightened. The caps were then tightened, and the vials were placed in an 80 °C water bath for 60 min and then allowed to cool to ambient temperature. Samples (25−300 μL) were directly injected into the SEC columns.

Analyses. Analysis by size-exclusion chromatography (SEC) was performed as described earlier.[4,7] Due to the low polymer concentrations combined with low molecular weights in many of the samples, in-line analysis by low-angle laser light scattering (LALLS) measurements was not possible in most of the cases. Instead, the elution curves obtained from the refractive index detector were processed (PCLALLS software) with a calibration curve obtained from a linear fit of data (log M *versus* elution volume) obtained earlier with partially depolymerized xanthans.[4] Reducing ends were analyzed by the Nelson reagent method.[22]

Electron Microscopy. Preparation of replicas for electron microscopy and electron microscopic investigations was carried out as described previously.[18,20]

Monte Carlo Simulations. The previous method for simulation of degradation of duplex and triplex polymers by random bond scissions in the individual chains[5] was extended to estimate the ratio of the molecular weight before and after a heat treatment involving a redistribution of chain fragments. Following the random attack at a given time, the molecular weight of the duplexes and released oligomer fragments according to the duplex stability criterium, $DP \leq DP_c$ (Figure 2), was taken as the weight average molecular weight prior to the heat treatment. The heat treatment and subsequent redistribution of chain fragments was implemented by removing all interstrand bonds (Figure 2), and $\bar{M}_w$ of the heat-treated sample was calculated by assuming that all chain fragments with $DP > DP_c$ were matched with an equally long chain. $\bar{M}_w$ of the duplex fraction after the heat treatment was calculated as twice that of the corresponding fraction in the strand-separated state, and the appropriate weighing using the oligomer fraction was carried out to get the ensemble averaged $\bar{M}_w$. Model monodisperse ensembles of 100 chains with initially $DP = 2000$ were used in the simulations. The simulations showed convergence within 5% for the largest ratio in $\bar{M}_w$(before)/$\bar{M}_w$(after) for more than 50 chains.

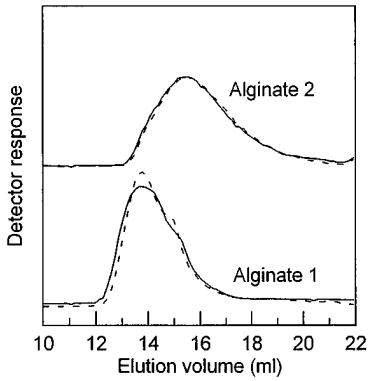

Figure 3. Size-exclusion chromatography profiles of untreated (—) and heat-treated (- - -) alginates.

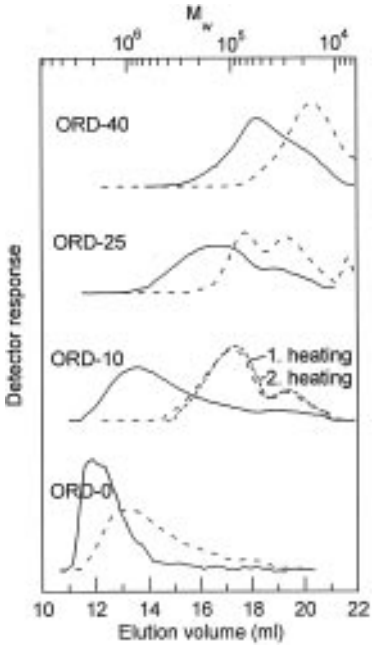

Figure 4. Size-exclusion chromatography profiles of untreated (—) and heat-treated (- - -) xanthans following depolymerization by H_2O_2/Fe^{2+} at 20 °C. Depolymerization times (hours) are indicated in the figure. The relationship between the molecular weight and the elution volume was established in a previous article.[4]

Results and Discussion

Control Samples (Single Stranded Polymers). Two different alginates were subjected to the heat treatment, and the corresponding elution profiles are given in Figure 3. In both cases the profiles are unaffected by the heat treatment, clearly demonstrating that no depolymerization occurs. Although the chemical composition of xanthan differs from that of alginate, it has been shown earlier[9] that these polymers do not differ very much in their susceptibilities toward depolymerization by free radical mechanisms, which will be the primary degradation process during the heat treatment.

Xanthans Depolymerized by H_2O_2/Fe^{2+} (Figures 4 and 5). A series of samples, depolymerized at 20 °C for 0−50 h were studied. Figure 4 shows results (chromatograms) obtained for samples ORD-0, ORD-10, ORD-25, and ORD-40, where the number corresponds to the depolymerization time (hours). The calculated values of $\bar{M}_w$ before and after the heat treatment are

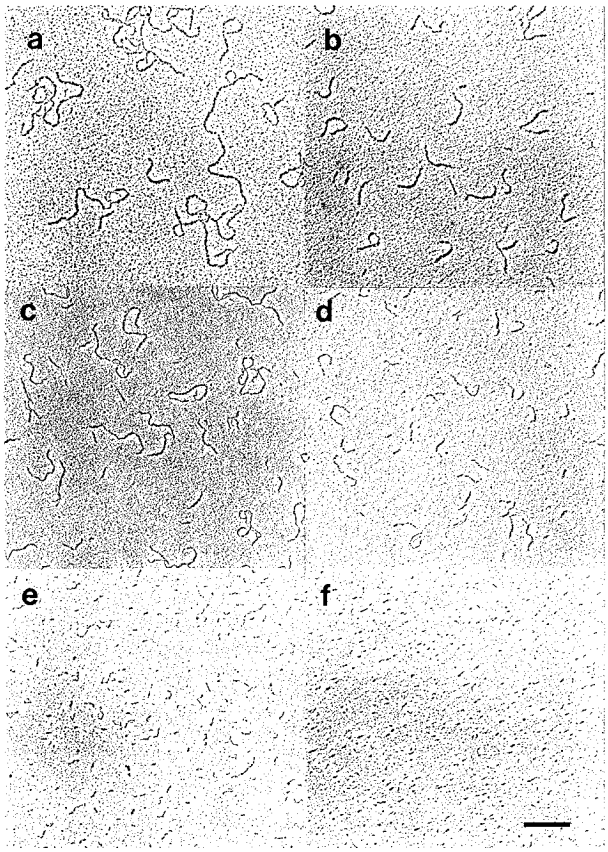

Figure 5. Electron micrographs of untreated (a, c, e) and heat-treated (b, d, f) xanthans following depolymerization by H_2O_2/Fe^{2+} at 20 °C. Depolymerization times are 0 h (a, b), 10 h (c, d), and 40 h (e, f). Scale bar: 200 nm.

Table 1. Change in $\bar{M}_w$ upon Heat Treatment (above T_m) of Partially Depolymerized Xanthans

	$\bar{M}_w$ ($\times 10^{-3}$)[b]			
sample code[a]	before heat treatment	after heat treatment	$\bar{M}_w$(after)/ $\bar{M}_w$(before)	$\bar{M}_w$(before)/ $\bar{M}_w$(after)
ORD-0	*c* (2500)	800 (660)	(0.26)	(3.4)
ORD-4	840 (850)	96	0.11	8.8
ORD-7	660 (640)	88 (84)	0.13 (0.13)	7.5 (7.6)
ORD-10[b]	580 (540)	102 (83)	0.18 (0.15)	5.7 (6.5)
ORD-15	296	68	0.23	4.4
ORD-25	160	54	0.34	3.0
ORD-40[b]	72	20	0.28	3.6
ORD-50	52	23	0.44	2.3
AH-22	1100 (2400)	820 (900)	0.75 (0.38)	1.3 (2.7)
AH-79	650 (780)	500 (670)	0.77 (0.86)	1.3 (1.2)
AH-199	360	240	0.67	1.5
SON-B	337	284	0.84	1.2
SON-2	170	98	0.58	1.7
SON-5	130	107	0.82	1.2

[a] ORD: degraded by H_2O_2/Fe^{2+} at 20 °C. AH: acid hydrolysis at 80 °C. SON: sonicated. [b] Numbers in parentheses are calculated by combing on-line LALLS data and RI data. [c] This sample eluted mainly in the void volume (see Figure 4) where the calibration line (log *M vs V*) is not properly defined.

given in Table 1, which also contains results obtained with other samples.

In addition to the shift toward higher elution volumes as a consequence of the depolymerization prior to the heat treatment, *i.e.* decrease in $\bar{M}_w$, a quite broad molecular weight distribution (MWD) could be observed for all of the untreated samples, except sample ORD-0, which eluted mainly in the void volume. The decrease in $\bar{M}_w$ resulting from the initial depolymerization is paralleled by a decrease in the contour lengths, as observed in the electron micrographs (Figures 5a,c,e). For samples depolymerized for 10 h or more a separate peak or shoulder eluting in the range 18.5−21 mL was obtained. This corresponds to the low-*M* fraction consisting of single-stranded fragments[4,7] that had been released during the degradation. A characteristic feature is that the amount of such fragments increases with increasing degradation times.[4,7]

For all samples the heat treatment resulted in a large shift in the MWD toward lower molecular weights. Except for sample ORD-0, the MWD of the heat-treated samples appears to be less broad, although the amount of material eluting in the low-*M* fraction has increased. The decrease in $\bar{M}_w$ was verified (qualitatively) in the electron micrographs (Figure 5), which showed that the heat-treated samples consisted almost exclusively of duplexes, but of reduced contour lengths. The EM results for sample ORD-40 (Figure 5e,f) are less conclusive because of the small molecular dimensions relative to the resolution of the method, and also because of the large content of single-stranded fragments in the untreated sample.

Heat treatment at a 10-fold lower xanthan concentration (0.07 mg/mL) yielded in all cases elution profiles identical to those obtained at higher concentrations (data not shown). This indicates that nonspecific aggregation effects, such as formation of larger structures, are minimized and do not influence the results.

Although polymers such as alginate (Figure 3) are not further degraded in the subsequent heat treatment, the presence of traces of, *e.g.*, Fe^{2+} in samples degraded by H_2O_2/Fe^{2+} might possibly lead to further depolymerization in the heat treatment. Sample ORD-10 was chosen for some additional control experiments. First, the number of reducing ends was analyzed, and the corresponding fraction of cleaved linkages in the glucan backbone (α) was calculated.[4] In accordance with earlier data,[4] this value was quite high, in this case 0.07, before the heat treatment. It should be noted that the high value of α (which equals $1/DP_n$) reflects two features, namely the "hidden" chain breaks within the duplex and the low-*M* fraction, which actually contains the major number of reducing ends.[7] A small increase in α to a value of 0.094, *i.e.* a factor of 1.3, was observed after the heat treatment. This change alone cannot explain the 7.5-fold decrease in $\bar{M}_w$ observed for this sample. A second heat treatment led to a further increase in α to 0.104. However, the elution profile was only marginally affected in this case (Figure 5). We therefore conclude that the heat treatment of samples initially depolymerized by H_2O_2/Fe^{2+} leads to negligible depolymerization and that the large decrease in M_w is caused by rearrangements of fragmented duplexes, *i.e.* a process corresponding to B → C → E in Figure 2.

The increase in the amount of low molecular weight fragments by the heat treatment is attributed to a certain hysteresis in the dissociation and reassociation of fragments with DP close to DP_c, since further depolymerization already has been ruled out.

Xanthans Depolymerized by Acid Hydrolysis (Figure 6). The changes in the elution profiles following heat treatment of partially acid hydrolyzed xanthans were generally smaller than for those depolymerized by H_2O_2/Fe^{2+} (Figure 4) and $\bar{M}_w$ decreased only a factor of 1.3−1.5 (Table 1). The chromatograms show that the main difference in the molecular weight distribution lies on the high-*M* side. However, the in-line calculated

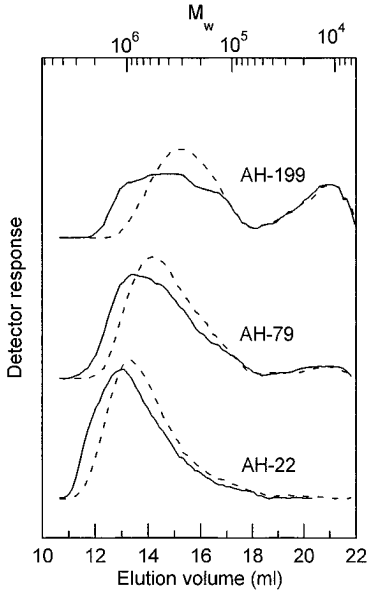

Figure 6. Size-exclusion chromatography profiles of untreated (—) and heat-treated (- - -) xanthans following depolymerization by hydrolysis in 0.1 M HCl at 80 °C. Depolymerization times (hours) are indicated in the figure.

molecular weights for samples AH-22 and AH-79 (based on the combined LALLS and RI data instead of the calibration curve) showed an upturn in the high-*M* region, indicating that aggregates were present. The changes in the elution profiles following heat treatment therefore suggest that the major process is dissolution of multichain aggregates rather than duplex rearrangements. This is supported by the observation that the low-*M* fraction, including the peak for single-stranded oligomers, is largely unaffected by the heat treatment. An exception to the latter was observed for a sample hydrolyzed for 247 h, where a large fraction of the population shifted from the high-*M* peak to the low-*M* peak, but with little change in the overall peak shapes. These data indicate that partially acid hydrolyzed xanthans undergo a much smaller degree of chain rearrangement as compared to xanthans degraded by H_2O_2/Fe^{2+}. The relatively small changes in the molecular weight distributions can largely be ascribed to the removal of high-*M* aggregates.

The absence of a large shift in the MWD seen for partially acid hydrolyzed, double-stranded xanthans contrasts the observations made for double-stranded xanthan degraded by H_2O_2/Fe^{2+} at 20 °C. We suggest that this may in part by due to a certain degree of duplex rearrangements actually occurring in the acid hydrolysis step, which is performed at 80 °C. The high temperature results in an increase in DP_c and contributes in addition to a reduction of the kinetic barriers which counteract chain rearrangements.

Xanthans Depolymerized by Sonication (Figure 7). Two of the sonicated samples behaved quite similarly to the acid-hydrolyzed samples, with only a 20% decrease in $\bar{M}_w$ upon the heat treatment (Table 1). One sample (SON-2) had a higher decrease. However, the presence of aggregates in the untreated samples cannot be ruled out in this particular sample. Whether the decrease in $\bar{M}_w$ seen in the two other samples is caused by a slight aggregation or by the introduction of a small amount of chain breaks within the duplex by the sonication procedure cannot be decided in the present study.

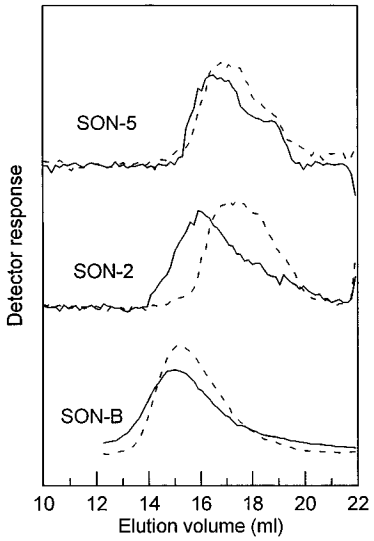

Figure 7. Size-exclusion chromatography profiles of untreated (—) and heat-treated (- - -) xanthan following depolymerization by sonication.

Monte Carlo Simulation of the Depolymerization and the Chain Rearrangements. The depolymerization and the idealized duplex rearrangements were simulated by extending the Monte Carlo simulation described earlier.[5] Following the introduction of randomly placed chain breaks in a duplex (DP = 2000), each individual fragment thus produced within the duplex (Figure 2, structure type B) was investigated with respect to chain length. For DP ≤ DP_c, the fragment was considered to dissociate from the parent duplex and remain single stranded. For DP > DP_c a rearrangement would take place where each fragment paired with another fragment of exactly the same length to produce a perfectly matched duplex (Figure 2, structure E). The weight average degree of polymerization or, equivalently, $\bar{M}_w$, was calculated before and after the rearrangement process for three values of DP_c (5, 10, and 15 glucose residues).

Figure 8a shows the ratio between the calculated $\bar{M}_w$ before and after the rearrangement process as a function of α (fraction of cleaved linkages per chain). Figure 8b shows the same data plotted as a function of the relative decrease in $\bar{M}_w$, *i.e.* $\bar{M}_{w,\alpha}/\bar{M}_{w,\alpha=0}$, resulting from the depolymerization *prior* to the heat treatment. For α = 0 and α = 1 the ratio approaches 1 since these cases represent an undegraded duplex and only single-stranded fragments, respectively. The increase in the ratio $\bar{M}_w$(heat-treated)/$\bar{M}_w$(untreated) for slightly depolymerized samples (α < 0.001) corresponds to the situation where few of the chain breaks actually lead to a scission of the duplex since the chain overlaps are generally larger than DP_c. For more extensive depolymerization this ratio reaches a maximum and then decreases again because additional chain breaks activate "hidden" breaks, since many of the chain overlaps now become shorter than DP_c. In the very late stages the release of single-stranded fragments also contributes to a decrease in the ratio, since the relative amount of remaining (metastable) duplexes decreases.

The maximum value of $\bar{M}_w$(heat-treated)/$\bar{M}_w$(untreated) is obtained for α values in the range 0.005−0.001, corresponding to $\bar{M}_{w,\alpha}/\bar{M}_{w,\alpha=0} = 0.5-0.6$. The maximal ratio increases with decreasing DP_c, and the corresponding value of α also increases slightly. A ratio of about 7 is observed for $DP_c = 5$.

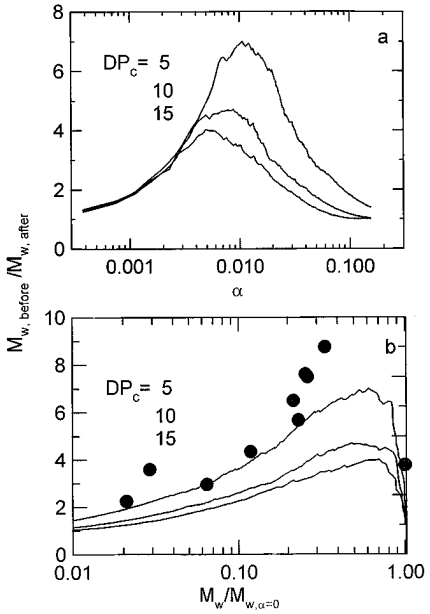

Figure 8. Results from a Monte Carlo simulation of the change in $\bar{M}_w$ following rearrangements of individual fragments within a metastable, partially depolymerized duplex structure to form perfectly matched duplexes for different values of the fraction of broken linkages (α). The simulation was carried out for three values of DP_c, the critical DP below which no duplex formation is allowed.

Figure 8b includes the experimental data obtained for xanthans depolymerized by H_2O_2/Fe^{2+}. The curve shape predicted in the simulations is indeed observed, although the data tend to lie above the upper line (DP_c = 5), particularly for values of $\bar{M}_{w,\alpha}/\bar{M}_{w,\alpha=0}$ in the range 0.1−0.5. This suggests that DP_c may be below 5 glucose residues in the present case (10 mM NaCl, 20 °C).

Conclusions. The depolymerization of double-stranded xanthan by H_2O_2/Fe^{2+} (at 20 °C) results in the formation of a metastable duplex stabilized by overlapping chain fragments. A heat treatment well above T_m results in a decrease in $\bar{M}_w$. The decrease was found to be largest (factor 7−9) for slightly depolymerized xanthan, whereas the change in $\bar{M}_w$ by the heat treatment decreased upon further depolymerization. This pattern was well reproduced by a simple Monte Carlo simulation, where the duplex stability is governed by the degree of chain scission (α) and the critical DP needed for maintaining a stable duplex.

For xanthan degraded by acid hydrolysis at high temperatures we suggest that the relatively small decrease in $\bar{M}_w$ (factor 1.3−1.5) upon heat treatment well above T_m is partly caused by chain rearrangements occurring during the hydrolysis because of the high temperature.

Acknowledgment. This work was partly supported by VISTA (grants V6312 and V6314), a research cooperation between the Norwegian Academy of Science and Letters and Statoil, and by the Norwegian Research Council (grant BT27472). M. Myhr and A-S. Ulseth are thanked for skillful technical assistance.

References and Notes

(1) Davison, P.; Mentzer, E. *Soc. Petrol. Eng. J.* **1982**, June, 353.
(2) Muller, G.; Lecourtier, J. *Carbohydr. Polym.* **1988**, *9*, 213.
(3) Christensen, B. E.; Smidsrød, O. *Carbohydr. Res.* **1991**, *214*, 55.
(4) Christensen, B. E.; Smidsrød, O. *Carbohydr. Res.* **1996**, *280*, 85.
(5) Stokke, B. T.; Christensen, B. E.; Smidsrød, O. *Macromolecules* **1992**, *25*, 2209.
(6) Christensen, B. E.; Knudsen, K. D.; Smidsrød, O.; Kitamura, S.; Takeo, K. *Biopolymers* **1993**, *33*, 151.
(7) Christensen, B. E.; Smidsrød, O.; Elgsaeter, A.; Stokke, B. T. *Macromolecules* **1993**, *26*, 6111.
(8) Christensen, B. E.; Smidsrød, O.; Stokke, B. T. *Front. Biomed. Biotechnol.* **1993**, *1*, 166.
(9) Hjerde, T.; Kristiansen, T. S.; Stokke, B. T.; Smidsrød, O.; Christensen, B. E. *Carbohydr. Polym.* **1994**, *24*, 265.
(10) Cantor, C. R.; Schimmel, P. R. *Biophysical Chemistry*; W. H. Freeman: San Francisco, 1980; p 1041.
(11) Applequist, J.; Damle, V. *J. Am. Chem. Soc.* **1965**, *87*, 1450.
(12) Milas, M.; Rinaudo, M. *Carbohydr. Res.* **1986**, *158*, 191.
(13) Oviatt, H. W.; Brant, D. A. *Int. J. Biol. Macromol.* **1993**, *15*, 3.
(14) Norton, I. T.; Goodall, D. M.; Frangou, S. A.; Morris, E. R.; Rees, D. A. *J. Mol. Biol.* **1984**, *175*, 371.
(15) Coviello, T.; Kajiwara, K.; Burchard, W.; Dentini, M.; Crescenzi, V. *Macromolecules* **1986**, *19*, 2826.
(16) Stokke, B. T.; Elgsaeter, A.; Brant, D. A.; Kitamura, S. *Macromolecules* **1991**, *24*, 6349.
(17) Stokke, B. T.; Elgsaeter, A.; Brant, D. A.; Kuge, T.; Kitamura, S. *Biopolymers* **1993**, *33*, 193.
(18) Stokke, B. T.; Brant, D. *Biopolymers* **1990**, *30*, 1161.
(19) Stokke, B. T.; Elgsaeter, A. *Micron* **1994**, *25*, 469.
(20) Stokke, B. T.; Elgsaeter, A.; Smidsrød, O. *Int. J. Biol. Macromol.* **1986**, *8*, 217.
(21) Skjåk-Braek, G.; Grasdalen, H.; Larsen, B. *Carbohydr. Res.* **1986**, *154*, 239.
(22) Hodge, J. N.; Hofreiter, B. T. *Methods Carbohydr. Chem.* **1962**, *1*, 386.

MA951445O